SCIENTIFIC REPORTS

OPEN

SUBJECT AREAS:
ULTRAFAST PHOTONICS
ULTRAFAST LASERS
SEMICONDUCTOR LASERS
APPLIED PHYSICS

Received
21 January 2014

Accepted
20 February 2014

Published
10 March 2014

Correspondence and requests for materials should be addressed to B.P.Z. (bzhang@xmu.edu.cn)

Spectral dynamics of picosecond gain-switched pulses from nitride-based vertical-cavity surface-emitting lasers

Shaoqiang Chen[1], Takashi Ito[1], Akifumi Asahara[1], Masahiro Yoshita[1], Wenjie Liu[2], Jiangyong Zhang[2], Baoping Zhang[2], Tohru Suemoto[1] & Hidefumi Akiyama[1]

[1]Institute for Solid State Physics, University of Tokyo, 5-1-5 Kashiwanoha, Kashiwa, Chiba 277-8581, Japan, [2]Department of Physics & Department of Electronic Engineering, Xiamen University, Xiamen 361005, Fujian, China.

Short pulses generated from low-cost semiconductor lasers by a simple gain-switching technique have attracted enormous attention because of their potential usage in wide applications. Therein, reducing the durations of gain-switched pulses is a key technical point for promoting their applications. Therefore, understanding the dynamic characteristics of gain-switched pulses is highly desirable. Herein, we used streak camera to investigate the time- and spectral-resolved lasing characteristics of gain-switched pulses from optically pumped InGaN single-mode vertical-cavity surface-emitting lasers. We found that fast initial components with ultra-short durations far below our temporal resolution of 5.5 ps emerged on short-wavelength sides, while the entire pulses were down-chirped, resulting in the simultaneous broadening of the spectrum and pulse width. The measured chirp characteristics were quantitatively explained using a single-mode rate-equation model, combined with carrier-density-dependent gain and index models. The observed universal fast short-wavelength components can be useful in generating even shorter pulses from gain-switched semiconductor lasers.

Low-cost, robust, compact, and short-pulse semiconductor lasers are on demand in many applications such as the next-generation high-density high-capacity three-dimensional optical storages[1–5] and bio-medical imaging[6,7]. The characteristic wide direct energy gap, high luminescence efficiency, and high stability of nitride semiconductors suggest that nitride-based semiconductor lasers can be used to achieve shorter-wavelength light sources[8–13]. Increasing attention has been devoted to pulse generation from nitride-based semiconductor blue lasers by gain-switching technique[14–17], which is a simple and inexpensive technique of short-pulse generation through direct modulation of semiconductor lasers. Pulse widths of gain-switched pulses range from several tens to several hundreds of picoseconds; to promote the application of gain-switched semiconductor lasers, shorter pulses with pulse widths on picosecond and subpicosecond scales are desirable. However, it is still a challenge to develop gain-switched pulse sources with picosecond- or subpicosecond-scale pulse widths.

One of the difficulties in obtaining short pulses from gain-switched semiconductor lasers is complex spectral dynamics that include nonlinear chirping (a phenomenon intrinsic to directly modulated semiconductor lasers), i.e., a dynamic shift of the peak emission wavelength during lasing, caused by the transient-carrier-density-change-induced index change in the active regions of semiconductor lasers. Nonlinear chirps may broaden the lasing spectrum and the output-pulse width of directly modulated semiconductor lasers, and thus, have so far attracted considerable attention[18–23]. Previously, we have studied the dynamics of nonlinear chirps of a gain-switched 1.55-μm single-mode distributed feedback laser diode (DFB-LD)[24,25]; we also demonstrated that nearly transform-limited sub-5-ps short pulses could be generated via spectral filtering technique from the short-wavelength side of highly chirped gain-switched pulses. These results indicated that a proper knowledge and control of chirp characteristics can help learn how to generate even shorter pulses by using gain-switched semiconductor lasers.

Besides the DFB-LD, another well-known single-mode laser is vertical-cavity surface-emitting laser (VCSEL)[26], which has the advantages of low laser threshold, wafer-scale processing, and the ability to form two-dimensional device arrays. Owing to the improved crystal growth and device-processing techniques, nitride-based single-mode VCSELs with blue- and green-region lasing wavelength have been demonstrated[17,27–29]. However, regarding the nitride-based VCSELs, transient characteristics of gain-switched pulses, including wavelength chirp during lasing, remain elusive.

In this paper, transient characteristics of gain-switched pulses from a single-mode gain-switched InGaN VCSEL were investigated via optical pumping and streak-camera direct observations. The time- and spectral-resolved streak-camera images of the gain-switched pulses demonstrated that, for high pump-power levels, the gain-switched pulses originate on short-wavelength side and have an initial duration much shorter than 5 ps, then broaden and simultaneously shift toward the long-wavelength side. The chirp was found to increase while the pulse width and pulse-delay time decreased with increasing pump power. The chirp, pulse width, and pulse-delay time exhibited saturation at high pump-power levels. These characteristics were satisfactorily explained by using a theoretical model with a single-mode rate equation that included carrier-density-dependent gain with saturation.

Results

Time- and spectral-resolved measurements of gain-switched pulses. Figure 1 shows the sample structure of InGaN VCSEL and the experimental setup. The vertical cavity of the sample consisted of three-period InGaN/GaN quantum wells and two Ta_2O_5/SiO_2 distributed Bragg reflectors (DBRs), with a cavity length of 2.3 μm, resulting in a cavity lifetime of 0.6 ps. Fabrication procedure of the VCSEL is given in the Supplementary Information. The sample was optically pumped with a 1-kHz, 400-nm, and 300-fs pulse laser beam with a beam size of ~50 μm and was focused on the sample surface by using an optical lens. This experimental setup demonstrated the simplicity of the gain-switching operation. The time-integrated emission spectra were measured by using a spectrometer system with a liquid nitrogen-cooled charge-coupled device (CCD). The time-resolved emission spectra were measured using a streak camera.

The time-integrated emission spectra obtained for various pump-power levels are shown in the upper panel of Fig. 1. Single-mode lasing at 444.5 nm was started for a pump-power value higher than 20.8 μW (henceforth, average power) and remained at the single mode even for elevated pump-power values. The enlarged lasing mode spectra, shown in the figure inset, disclose that the blue shift and spectral broadening on the short-wavelength side occur at elevated pump-power values. The spectral resolution in Fig. 1 is 0.15 nm.

Figure 2 shows the time- and spectral-resolved streak-camera images of the VCSEL gain-switched output pulses for various pump-power levels (additional images are provided in the Supplementary Information). The system's spectral resolution was 0.15 nm. The spectrally integrated waveforms of the pulses are shown in the bottom panel of Fig. 2. The measured 5.5-ps width of the 300-fs pump pulse indicates that the system resolution of the present streak camera is 5.5 ps. The pulse width and delay time of the VCSEL gain-switched pulses are gradually reduced as the pump power increases. This observed dependence of the delay time and pulse width on the power is typical for gain-switched pulses. The measured shortest pulse width is ~10 ps (including the 5.5-ps resolution width) with a delay time of 16 ps. As the pulse width and delay time of gain-switched pulses decrease with increasing pump power, the initial transient spectral broadening on the short-wavelength side of the pulses appears gradually and becomes significant at elevated pump-power values. This spectral broadening observed on the short-wavelength side by using a streak camera is in good agreement with the results of time-integrated spectroscopy shown in Fig. 1.

To analyze the spectral dynamics of gain-switched pulses, a streak-camera image, obtained for the pump power of 221.7 μW, is replotted in Fig. 3(a) after normalizing with respect to wavelength; this figure discloses a clear wavelength dependence of the pulse width and delay time (the streak-camera images before and after normalization are shown in Supplementary Information). The delay time and pulse width of the pulses at each wavelength, extracted from the streak-camera images of gain-switched pulses, are shown in Fig. 3(b).

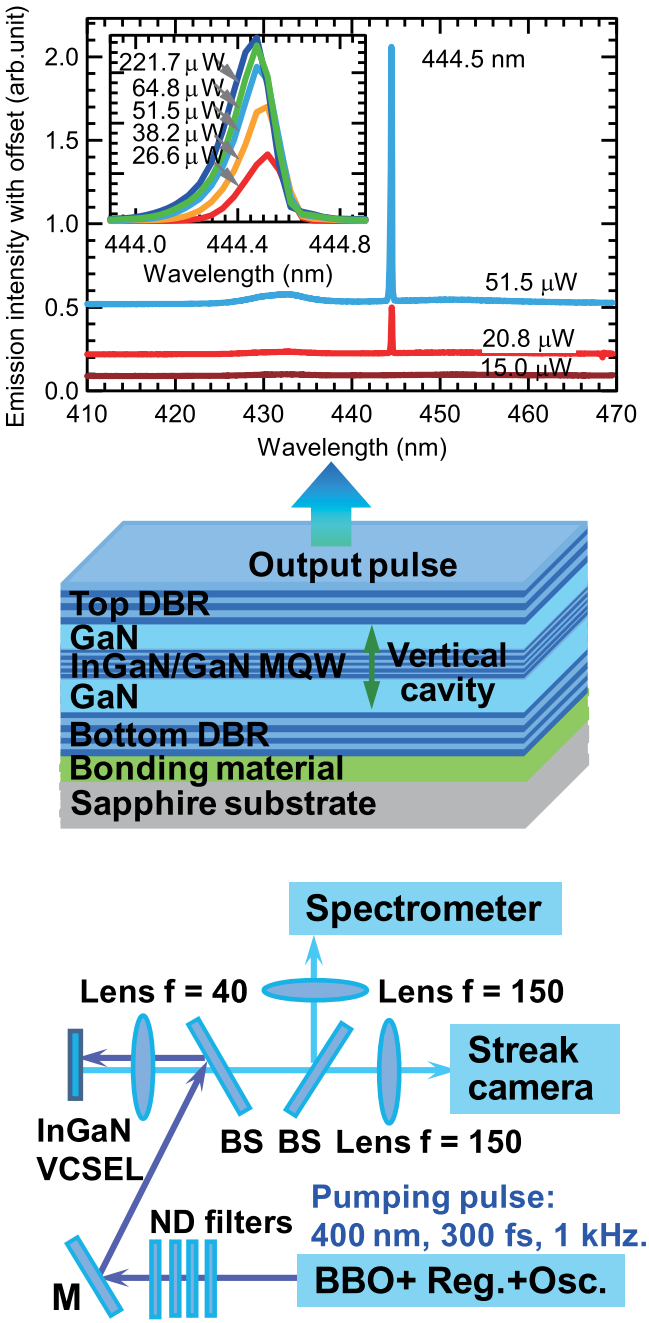

Figure 1 | Schematic diagram of experimental setup and sample structure. Top panel shows time-integrated lasing spectra of gain-switched InGaN vertical-cavity surface-emitting laser (VCSEL) for different pump powers. Inset shows enlarged lasing spectra. Note the spectral broadening toward short-wavelength side as the pump power is increased. ND filter: neutral density filters; BS: beam splitter; M: mirror; Osc: oscillator; Reg: regenerative amplifier; BBO: β -BaB_2O_4 (BBO) crystal.

Figure 3(c) shows three examples of the extracted pulse waveforms, for different wavelengths. From these results, it can be seen that the pulses on the short-wavelength side are much shorter than those on the long-wavelength side.

Figure 3(b) shows that, for short wavelength below 444.4 nm, the measured pulse widths are very short and almost limited by the system resolution of 5.5 ps (Fig. 3(c) also shows that the pulse shape of the pulses on short wavelength side overlaps well with the system response), and the delay time increases almost linearly with increasing wavelength (linear down chirp) with a slope (i.e., wavelength

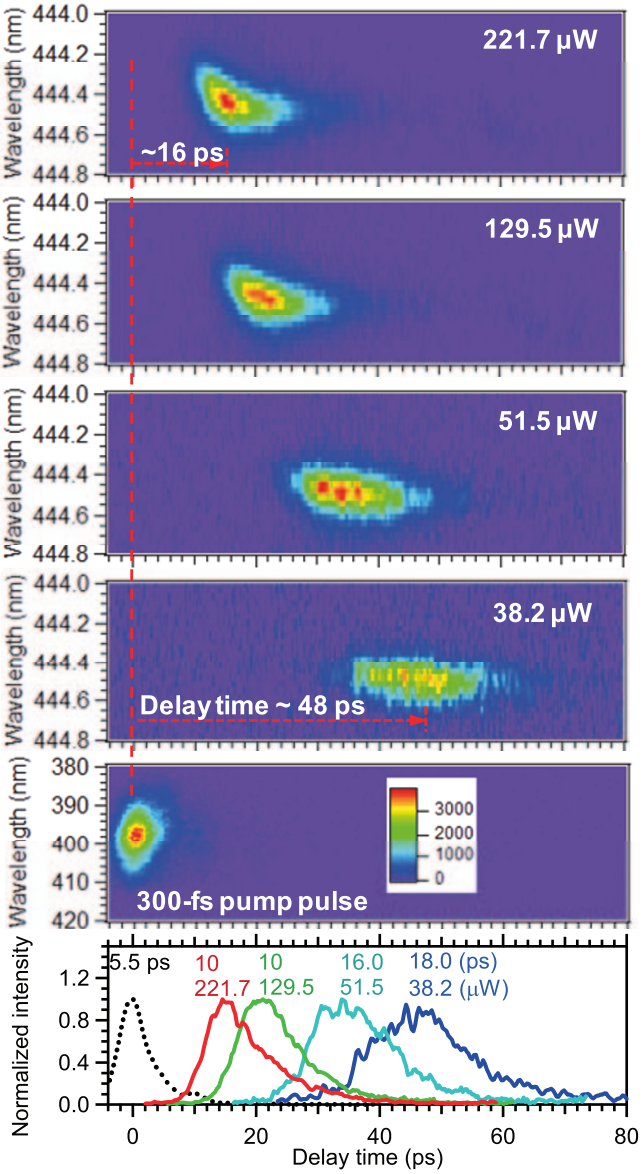

Figure 2 | Streak-camera images and the corresponding spectral-integrated waveforms of output pulses of gain-switched InGaN vertical-cavity surface-emitting laser (VCSEL) for various pump power values. Note the power dependency of spectral broadening toward short-wavelength side, pulse width, and delay time of pulses.

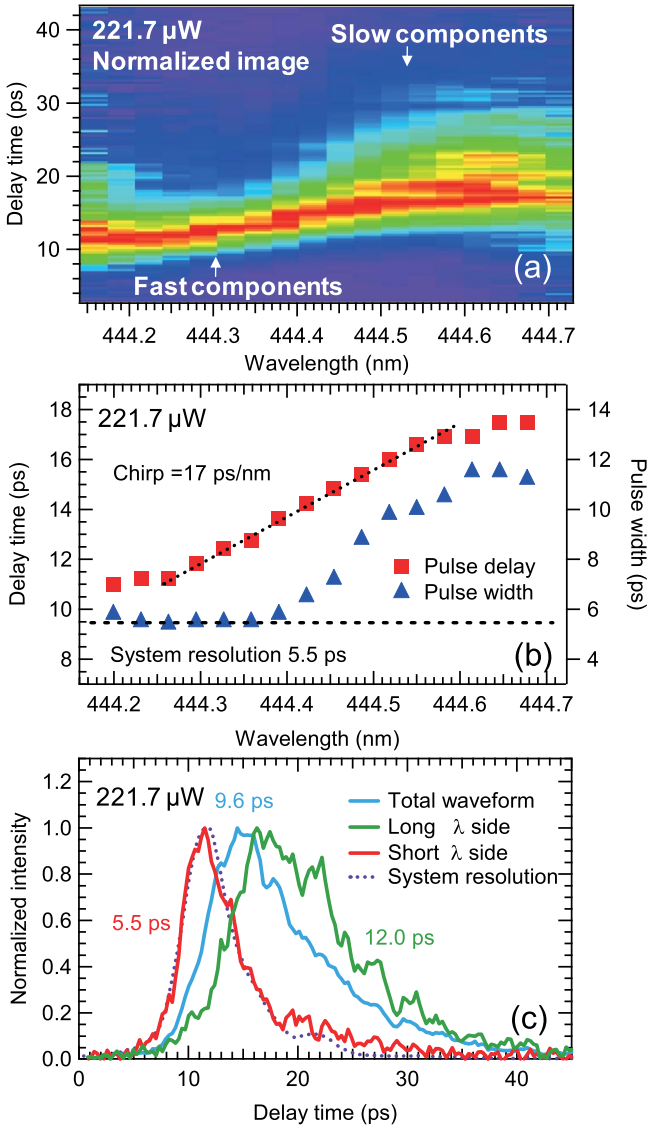

Figure 3 | (a) Normalized streak-camera image of gain-switched output pulses of InGaN vertical-cavity surface-emitting laser (VCSEL) with pump power of 221.7 μW. Note the wavelength dependence of pulse widths. (b) Delay times and pulse-width values of pulses for each wavelength extracted from (a). (c) Pulse waveforms of the total spectrum, short-wavelength side and long-wavelength side of pulses with pump power of 221.7 μW. Note the overlap of pulse waveforms on short-wavelength side and those of pump pulses (system's response).

chirp) of 17 ps/nm. In contrast, for wavelengths longer than 444.4 nm, the pulse width increases significantly with increasing wavelength (Fig. 3(c) also shows that the pulses on long wavelength side have longer pulse width and delay time than the pulses on short wavelength side). The streak-camera image in Fig. 3(a) shows that there is a common long tail (slow component) at the end of the pulse for wavelengths longer than 444.4 nm. This long tail was found to have a decay time of 8 ps, independent of pump power (see the Supplementary Information).

Quantitative simulation of wavelength-chirp dynamics. Figures 4(a) and (b) show the magnitudes of the wavelength chirps and the delay times of the gain-switched pulses for various pump powers extracted from the time-resolved streak-camera images. The chirp (in units of nm/ps) increases and the delay time decreases gradually with increasing pump power, followed by the saturation of both the chirp and delay time at elevated pump-power values.

These power-dependent chirp characteristics and pulse delay times of the gain-switched pulses were quantitatively simulated with a single-mode rate-equation model[30,31] that combined a carrier-density-dependent gain with saturation[30–32] and an α-parameter, giving a chirp that is proportional to the gain[18–23]:

$$\frac{dn}{dt} = \eta\frac{P(t)}{h\nu mA} - \frac{\Gamma}{m}v_g g(n,s)\,s - \frac{n}{\tau_r} \quad (1)$$

$$\frac{ds}{dt} = \Gamma v_g g(n,s)\,s - \frac{s}{\tau_p} + m\beta\frac{n}{\tau_r} \quad (2)$$

$$g(n,s) = \frac{g_0(n-n_0)}{[1+g_0(n-n_0)/g_s](1+\varepsilon s)} \quad (3)$$

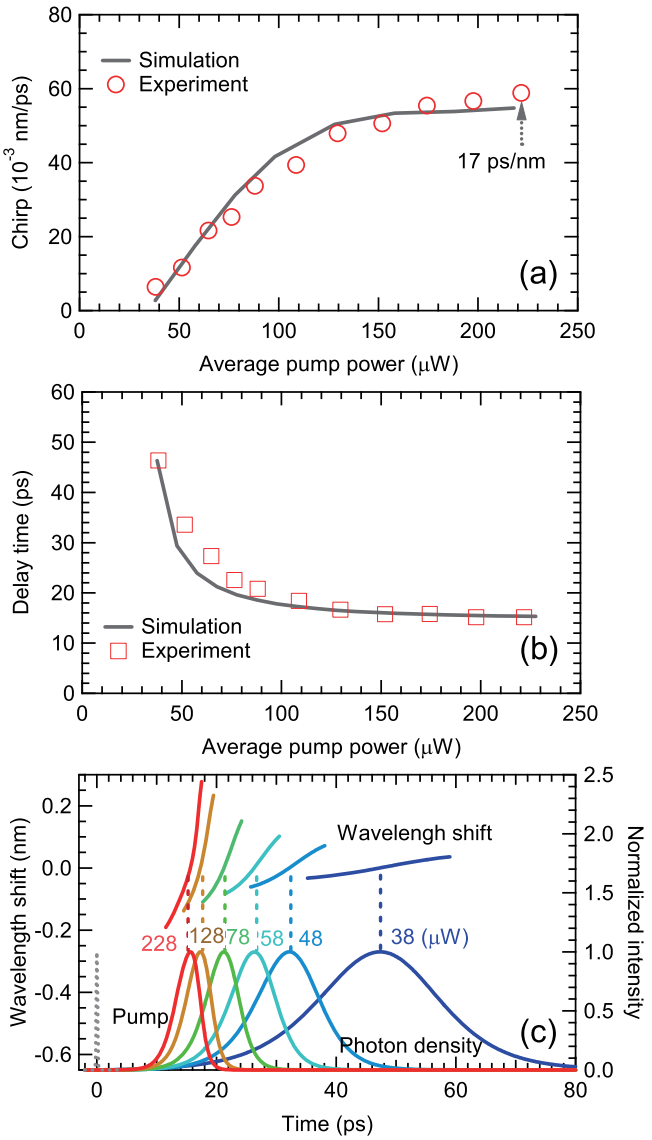

Figure 4 | (a) Experimental and simulation results of chirps of gain-switched pulses as a function of pump power. (b) Experimental and simulation results of pulse delay times of gain-switched pulses as a function of pump power. (c) Simulation results of temporal evolution of transient lasing-wavelength shift and output photon density of InGaN vertical-cavity surface-emitting laser (VCSEL) during gain switching with various pump powers. Slopes of simulated wavelength shifts with different pump powers are summarized in (a) and delay times of simulated pulses are summarized in (b).

$$\Delta\lambda = \frac{\lambda^2}{c}\frac{\alpha}{4\pi}\frac{1}{s}\frac{ds}{dt} \simeq \frac{\lambda^2}{c}\frac{\alpha}{4\pi}\left[\Gamma v_g g(n,s) - \frac{1}{\tau_p}\right] \quad (4)$$

Here, λ is the wavelength of the lasing mode, $\Delta\lambda$ is the wavelength shift, α is the linewidth enhancement factor, s is the two-dimensional photon density for all active layers, n is the two-dimensional carrier density in one quantum well, and $g(n,s)$ is the carrier-density- and photon-density-dependent material gain. The parameter g_s is the saturated material gain of the InGaN quantum well, τ_p is the cavity lifetime, and $P(t)$ is the transient pump power given by a Gaussian function with an full width at half maximum (FWHM) of 0.3 ps. Definitions of other parameters are summarized in Table 1.

Figure 4(c) shows the simulated temporal evolution of wavelength shift (top) and the corresponding photon density (bottom) during pulse generation, for various pump power values. Note that the initial wavelength shifts (or broadens) toward the short-wavelength side as the pump power increases. This result is in a good agreement with the experimentally observed spectral broadening that occurs for increasing pump power. Note also that the slope of the wavelength shift (namely, the chirp) increases, while the pulse width and delay time decrease with increasing pump power. This is also in a good agreement with the observed experimental results. For high pump-power values, the chirp, the delay time, and the pulse width are saturated. These saturations can be explained by the saturation of gain $g(n,s)$ (i.e., the saturation gain g_s) in Eqs.(3) and (4) for high pump-power values. High saturation gain is an important factor for short-pulse generation by gain-switching.

Table 1 | Definitions and values of simulation parameters

Parameters	Definitions	Values
m	Quantum well number	3
A	Lasing area	2.5×10^{-5} cm^2
$h\nu$	Photon energy	3.1 eV
η	Absorption efficiency	0.4
Γ	Confinement factor	4.6×10^{-3}
v_g	Group velocity	1.1×10^{-2} cm/ps
τ_r	Carrier lifetime	5 ns
τ_p	Cavity lifetime	0.6 ps
α	Linewidth-enhancement factor	6.2
β	Spontaneous emission coupling factor	3.0×10^{-2}
g_s	Saturated gain	4.9×10^4 cm^{-1}
g_0	Differential gain	2.0×10^{-10} cm
n_0	Transparent carrier density	2.0×10^{12} cm^{-2}
ε	Gain compression factor	2.0×10^{-16} cm^2

Discussion

Based on the above results, the dynamics underlying the generation of short pulses under conditions of high pump-power values can be explained as follows: during the initial stage of pulse lasing, the transient carrier density in the cavity is very high, and consequently the transient refractive index is low. Thus, pulse lasing starts at a short wavelength with a high gain, causing a short pulse width. As the carriers are consumed, the pulse lasing shifts toward the long-wavelength side with a linear speed of 58 pm/ps (i.e., the chirp, inversely 17 ps/nm). The measured total pulse width of 10 ps for the gain-switched pulses in high pump-power conditions was the integration of the fast chirped component on the short-wavelength side and the additional slow component on the long-wavelength side.

Note that the essential results shown above are very similar to, and are probably the same as, the previously observed results for a single-mode DFB-LD[24,25], where the pulse was short and down-chirped on the short-wavelength side, and was mixed with very slow components on the long-wavelength side. In the DFB-LD experiment, pumping was achieved by much longer nanosecond-scale electrical pulses, and the slow long-wavelength component was ascribed to the near steady state, or pedestal, lasing. However, because we used femtosecond optical pumping in the present study, the slow long-wavelength component cannot be ascribed to steady-state components as in the nanosecond-pumped DFB-LD.

The origin of the slow long-wavelength component in the present study is not known yet. Nevertheless, a spectral filtering technique should be useful in eliminating it and in extracting only the fast chirped component in the short wavelength[24,25]. According to the measured chirp of 17 ps/nm and the spectral width of 0.3 nm, the pulse width after the spectral filtering will be 5 ps. A chirp-compression technique should then be useful for further reducing the pulse width.

In summary, the spectral dynamics of the picosecond gain-switched pulses from a single-mode optically pumped InGaN VCSEL were investigated by using streak-camera direct observations and theoretical simulations. The fast short-wavelength components showed pump-power-dependent wavelength chirp with a maximal value of 17 ps/nm. This chirp and an additional slow long-wavelength component were the main reasons for the broadening of the output pulse width. Even shorter pulses could be generated via spectral filtering and proper chirp compensations. The simulation suggested that an increased saturation gain, for example by increasing the number or the thickness of InGaN layers, should make the short-wavelength component faster. The generation dynamics of picosecond gain-switched pulses from the InGaN VCSEL revealed in this study is expected to provide an important reference for the understanding of the gain-switching mechanism and generation of short gain-switched pulses with nitride-based and other-material-based VCSELs.

Methods

Fabrication of sample. The InGaN multiple quantum wells were grown on sapphire substrates by using metal-organic chemical vapor deposition. First, the bottom DBRs were fabricated on the sample surface by electron-beam-evaporation technique. Then, the sample with the bottom DBR was bonded to another sapphire substrate, and the substrate that was used for the growth was removed by the laser-liftoff technique. Following this, the top DBR was fabricated on the sample. Detailed description of the fabrication process can be found in the Supplementary Information.

Characterization of sample. The pump light source was a regenerative amplifier (Spectra Physics, Spitfier), producing 1-kHz, 120-fs pulses at 800 nm, seeded by a mode-locked Ti:sapphire laser (Spectra Physics, TSUNAMI 3160C). The VCSEL was optically excited by impulsive fs pulses at 400 nm, which were obtained by taking the second harmonics of the 800-nm fundamental wave with a β -BaB_2O_4 (BBO) crystal. The pump laser beam with a beam size of $\sim$50 μm was focused on the sample surface by using an optical lens. The time-resolved emission spectra were measured by a streak camera (Hamamatsu C5680) combing a monochromator. All the experiments were performed at room temperature.

Simulation. Table 1 summarizes the definitions and values of all the parameters used for simulation. Therein, differential gain g_0, gain compression factor ε, saturated material gain g_s, and line enhancement factor α are the main fitting parameters. The used values of these main parameters for the best simulations of the experimental results were in very good agreement with the results of theoretical calculations and experiments in the references[33–37]. Other parameters are device parameters or fixed values obtained from references or experimental results.

1. Parthenopoulos, D. A. & Rentzepis, P. M. Three-dimensional optical storage memory. *Science* **245**, 843–845 (1989).
2. Keller, U. Recent developments in compact ultrafast lasers. *Nature* **424**, 831–838 (2003).
3. Walker, E. *et al.* Terabyte recorded in two-photon 3D disk. *Appl. Opt.* **47**, 4133–4139 (2008).
4. Anscombe, N. Data storage: Blue laser battle. *Nat. Photonics* **2**, 393 (2008).
5. Tashiro, S. *et al.* Volumetric optical recording using a 400 nm all-semiconductor picosecond laser. *Appl. Phys. Express* **3**, 102501 (2010).
6. Kawakami, R. *et al.* Visualizing hippocampal neurons with in vivo two-photon microscopy using a 1030 nm picosecond pulse laser. *Sci. Rep.* **3**, 1014 (2013).
7. Yokoyama, H. *et al.* Two-photon bioimaging with picosecond optical pulses from a semiconductor laser. *Opt. Express* **14**, 3467–3471 (2006).
8. Ponce, F. A. & Bour, D. P. Nitride-based semiconductors for blue and green light-emitting devices. *Nature* **386**, 351–359 (1997).
9. Rigby, P. The future is looking blue. *Nature* **384**, 610 (1996).
10. Gee, S. & Bowers, J. E. Ultraviolet picosecond optical pulse generation from a mode-locked InGaN laser diode. *Appl. Phys. Lett.* **79**, 1951 (2001).
11. Vasil'ev, P. P. *et al.* Mode locking in monolithic two-section InGaN blue-violet semiconductor lasers. *Appl. Phys. Lett.* **102**, 121115 (2013).
12. Kuramoto, M. *et al.* Enormously high-peak-power optical pulse generation from a single-transverse-mode GaInN blue-violet laser diode. *Appl. Phys. Lett.* **96**, 051102 (2010).
13. Saito, K. *et al.* Mode locking of an external-cavity bisection GaInN blue-violet laser diode producing 3 ps duration optical pulses. *Appl. Phys. Lett.* **96**, 031112 (2010).
14. Marinelli, C. *et al.* Gain-switching of GaInN multiquantum well laser diodes. *Electron. Lett.* **36**, 83–84 (2000).
15. Kono, S. *et al.* 12 W peak-power 10 ps duration optical pulse generation by gain switching of a single-transverse-mode GaInN blue laser diode. *Appl. Phys. Lett.* **93**, 131113 (2008).
16. Oki, T. *et al.* Generation of over 10-W peak-power picosecond pulses by a gain-switched AlGaInN-based self-pulsating laser diode. *Appl. Phys. Express* **2**, 032101 (2009).
17. Chen, S. Q. *et al.* Blue 6-ps short-pulse generation in gain-switched InGaN vertical-cavity surface-emitting lasers via impulsive optical pumping. *Appl. Phys. Lett.* **101**, 191108 (2012).
18. Lin, C., Lee, T. P. & Burrus, C. A. Picosecond frequency chirping and dynamic line broadening in InGaAsP injection lasers under fast excitation. *Appl. Phys. Lett.* **42**, 141–143(1983).
19. Linke, R. A. Modulation induced transient chirping in single frequency lasers. *IEEE J. Quantum Elect.* **QE-21**, 593–597 (1985).
20. Pataca, D. M. *et al.* Gain-switched DFB lasers. *Journal of Microwaves and Opto.* **1**, 46–63 (1997).
21. Koch, T. L. & Linke, R. A. Effect of nonlinear gain reduction on semiconductor laser wavelength chirping. *Appl. Phys. Lett.* **48**, 613–615 (1986).
22. Sato, K., Kuwahara, S. & Miyamoto, Y. Chirp characteristics of 40-Gb/s directly modulated distributed-feedback laser diodes. *J. Lightwave Technol.* **23**, 3790–3797 (2005).
23. Consoli, A. Tijero, J. M. G. & Esquivias, I. Time resolved chirp measurements of gain switched semiconductor laser using a polarization based optical differentiator. *Opt. Express* **19**,10805–10812 (2011).
24. Chen, S. Q. *et al.* Sub-5-ps optical pulse generation from a 1.55-μm distributed-feedback laser diode with nanosecond electric pulse excitation and spectral filtering. *Opt. Express* **20**, 24843–24849 (2012).
25. Chen, S. Q. *et al.* Dynamics of short-pulse generation via spectral filtering from intensely excited gain-switched 1.55-μm distributed-feedback laser diodes. *Opt. Express* **21**, 10597–10605 (2013).
26. Iga, K. Surface-emitting laser–Its birth and generation of new optoelectronics field. *IEEE J. Sel. Top. Quant.* **6**, 1201–1215(2000).
27. Krestnikov, I. L. *et al.* Room-temperature photopumped InGaN/GaN/AlGaN vertical-cavity surface-emitting laser. *Appl. Phys. Lett.* **75**, 1192–1194 (1999).
28. Someya, T. *et al.* Room temperature lasing at blue wavelengths in gallium nitride microcavities. *Science* **285**, 1905–1906 (1999).
29. Jiang, H. & Lin, J. Semiconductor lasers: Expanding into blue and green. *Nat. Photonics* **5**, 521 (2011).
30. Chen, S. Q. *et al.* Analysis of gain-switching characteristics including strong gain saturation effects in low-dimensional semiconductor lasers. *Jpn. J. Appl. Phys.* **51**, 098001 (2012).
31. Chen, S. Q. *et al.* Gain-switched pulses from InGaAs ridge-quantum-well lasers limited by intrinsic dynamical gain suppression. *Opt. Express* **21**, 7570–7576 (2013).
32. Ito, T. *et al.* Transient hot-carrier optical gain in a gain-switched semiconductor laser. *Appl. Phys. Lett.* **103**, 082117 (2013).
33. Domen, K. *et al.* Gain analysis for surface emission by optical pumping of wurtzite GaN. *Appl. Phys. Lett.* **69**, 94–96 (1996).
34. Chow, W. W. & Koch, S. W. Semiconductor-Laser Fundamentals: *Physics of the Gain Materials* (Springer, 1999).
35. Gan, K. G. & Bowers, J. E. Measurement of gain, group index, group velocity dispersion, and linewidth enhancement factor of an InGaN multiple quantum-well laser diode. *IEEE Photon. Technol. Lett.* **16**, 1256–1258 (2004).
36. Renzoni, F., Donegan, J. F. & Patterson, C. H. Optical gain and linewidth enhancement factor in bulk GaN. *Semicond. Sci. Technol.* **14**, 517–520 (1999).
37. Park, S. H. & Chuang, S. L. Linewidth enhancement factor of wurtzite GaN/AlGaN quantum-well lasers with spontaneous polarization and piezoelectric effects. *Appl. Phys. A* **78**, 107–111 (2004).

Acknowledgments

This work was partially supported by MEXT KAKENHI (No. 20104004, 20104006), JSPS KAKENHI (No. 23360135), the Photon Frontier Network Program of MEXT, and JST-CREST.

Author contributions

H.A., M.Y. and S.C. conceived the project. W.L., J.Z. and B.Z. fabricated the sample. S.C., T.I., A.A. and T.S. performed the characterizations. S.C. and M.Y. performed the simulations. S.C. and H.A. analyzed the results and wrote the paper. All authors joined the discussion and commented on the manuscript.

Additional information

Supplementary information accompanies this paper at http://www.nature.com/scientificreports

Competing financial interests: The authors declare no competing financial interests.

How to cite this article: Chen, S.Q. *et al.* Spectral dynamics of picosecond gain-switched pulses from nitride-based vertical-cavity surface-emitting lasers. *Sci. Rep.* **4**, 4325; DOI:10.1038/srep04325 (2014).

This work is licensed under a Creative Commons Attribution-NonCommercial-NoDerivs 3.0 Unported license. To view a copy of this license, visit http://creativecommons.org/licenses/by-nc-nd/3.0